Qualitative Chemical Analysis with Novel Structural Interpretations of Kyselina 2-Naftalensulfonova

R. Mini
Department of Physics and Research Centre, Women's Christian College, Nagercoil 629 001, TamilNadu, INDIA

T. Joselin Beaula
Department of Physics and Research Centre, Women's Christian College, Nagercoil 629 001, TamilNadu, INDIA

V. Bena Jothy
Department of Physics and Research Centre, Women's Christian College, Nagercoil 629 001, TamilNadu, INDIA

Abstract – Kyselina 2-naftalensulfonova (KNS) derivatives have been focused in the past decades due to their remarkable biological and pharmacological activities. Molecular geometry of KNS has been evaluated and compared with XRD data while the crystalline nature of the compound has been confirmed by PXRD study. Fourier Transform Infrared and FT-Raman spectra of the nonlinear optical material KNS were recorded and analyzed. Detailed interpretations of the vibrational spectra were carried out with the aid of normal coordinate analysis followed by scaled quantum mechanical force field methodology. Molecular orbital contributions have been investigated by TDOS and βDOS. Antimicrobial studies confirm the antibacterial effects. Molecular docking was performed for the different receptors for calculating binding affinities and predicting binding sites.

Index Terms – Vibrational spectra; PXRD, TDOS-βDOS; Molecular Docking.

1. INTRODUCTION

Bioactive substances are growing interest with a wide range in agrochemicals pharmaceuticals and polymers. This serves as an encouraging area with full refinement, which has emerged in modern research yielding more and more novel results, designed to change the resources of bioactive substances and improve their synthesis [1]. Kyselina 2-naftalensulfonova (KNS) and its derivatives are the most important class of organic compounds which are biologically, pharmaceutically and industrially useful compounds.

Chemical industrial processes are applied widely in concrete finishing, industrial textile processing, tanning of hides, manufacture of agrochemicals etc[2-4]. Literature survey reveals that neither quantum chemical calculations nor vibrational analysis of KNS have been reported yet. This inadequacy observed in literature has paved a way to undergo computational studies via Gaussian'09 package while experimental research provided detailed structural property assignments with the aid of FT-IR, FT-Raman, UV–visible and biological significance via molecular docking simulations.

2. EXPERIMENTAL DETAILS

FT-IR and FT-Raman spectra were recorded using PerkinElmer one: FT-IR Spectrometer and Bruker RFS 27: Stand alone FT-Raman Spectrometer with resolution of 1 and 2 cm^{-1}respectively. UV–visible absorption spectrum of the sample was measured, using UV–vis JASCO (V-570) UV/VIS/NIR spectrometer. Antimicrobial activities have been performed by Kirby-Bauer method.

3. COMPUTATIONAL DETAILS

Density Functional Theoretical (DFT) computations havebeen carried out using Gaussian'09 program package [5] at B3LYP/6-311++G(d,p) level. Characterization of normal modes using potential energy distribution (PED) have been performed with MOLVIB - 7.0 written by Sundius [6,7]. To improve agreement between predicted and observed frequencies, the computed harmonic frequencies have been scaled according to SQMFF procedure [8]. Cartesian representation of force constants have been transferred to non-redundant set of symmetry coordinates, chosen in accordance with the recommendations of Pulay et al. [9]. Auto Dock 4 (Version 1.5.6 revision 30) with the Lamarckian genetic algorithm has been performed docking studies [10].

4. RESULTS AND DISCUSSION

4.1 Structural properties

To confirm crystal structure, powder samples were analyzed by powder X-ray diffraction whereinthe powder samples were subjected to intense X-rays of 1.5418 Å andthe resulting powder X-ray diffraction pattern is shown in Fig.1. Obtained two-theta values were used for indexing by using the JCPDS (CARD NO: 351828) software package. Lattice parameters obtained are a= 15.20 Å, b= 16.54 Å, c=7.84 Å. Optimized Structural parameters of KNS calculated using DFT/B3LYP with 6-31++G(d,p) basis set have been listed in Table.1and the

molecular structure with Global minimum energy (-1009.8684 a.u.) is shown in Fig.2.

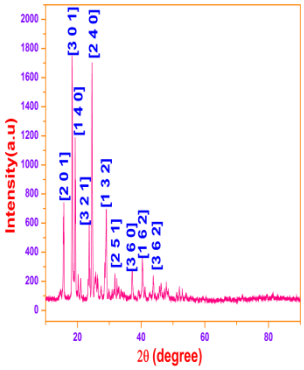

Fig.1 Powder XRD pattern of KNS

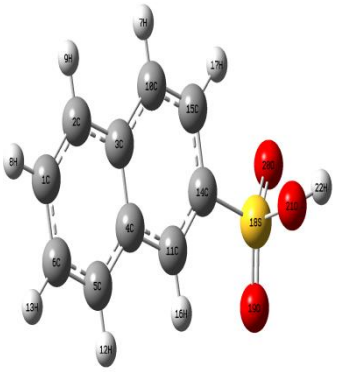

Fig.2 Optimized structure

Table:1 Optimized Bond lengths (Å) , Bond angles (°) and Dihedral angle(°)of KNS by b3lyp/6-31g(d,p)basis sets along with XRD data.

Bond Length	Theo. (Å)	Bond angle	Theo. (°)	Dihedral angle (°)	Theo. (°)
C_1-C_2	1.3769	C_1-C_2-C_6	120.5167	C_6- C_1-C_2-C_3	-0.0616
C_1- C_6	1.4163	C_2-C_1-H_8	119.9697	C_6- C_1-C_2- H_9	179.9099
C_1-H_8	1.0859	C_6-C_1-H_8	119.5136	H_8- C_1-C_2-C_3	179.9814
C_2-C_3	1.4196	C_1-C_2-C_3	120.6995	H_8- C_1-C_2- H_9	-0.047
C_2-H_9	1.0865	C_1-C_2-H_9	120.4473	C_2- C_1-C_6- C_5	0.033
C_3-C_4	1.4336	C_3- C_2 -H_9	118.8532	C_2- C_1-C_6- H_{13}	-179.9385
C_3-C_{10}	1.4228	C_2-C_3-C_4	118.7315	H_8- C_1- C_6- C_5	179.9901
C_4-C_5	1.4206	C_2-C_3 -C_{10}	122.1672	H_8- C_1- C_6- H_{13}	0.0186
C_4-C_{11}	1.419	C_4- C_3-C_{10}	119.1006	C_1-C_2-C_3- C_4	-0.0036
C_5-C_6	1.3761	C_3-C_4 -C_5	119.206	C_1-C_2-C_3-C_{10}	179.6873
C_5-H_{12}	1.0864	C_3-C_4-C_{11}	118.988	H_9-C_2-C_3- C_4	-179.9756
C_6-H_{13}	1.0856	C_5 -C_4-C_{11}	121.8059	H_9-C_2-C_3- C_{10}	-0.2847
H_7-C_{10}	1.0863	C_4 - C_5 - C_6	120.5743	C_2-C_3- C_4- C_5	0.0958
C_{10}-C_{15}	1.3734	C_4 - C_5 - H_{12}	118.8081	C_2-C_3- C_4-C_{11}	-179.9747
C_{11}-C_{14}	1.3755	C_6 -C_5 - H_{12}	120.6176	C_{10}-C_3- C_4- C_5	-179.6047
C_{11}-H_{16}	1.0849	C_1-C_6 -C_5	120.2719	C_{10}-C_3- C_4- C_{11}	0.3248
C_{14}-C_{15}	1.4169	C_1-C_6 - H_{13}	119.6287	C_2-C_3- C_{10}- H_7	-0.3481
C_{14}-S_{18}	1.782	C_5 - C_6- H_{13}	120.0994	C_2-C_3- C_{10}- C_{15}	-179.9355
C_{15}-H_{17}	1.084	C_3- C_{10}- H_7	118.7998	C_4- C_3- C_{10}-H_7	179.3416
S_{18}-O_{19}	1.4575	C_3- C_{10}- C_{15}	121.1942	C_4- C_3- C_{10}-C_{15}	-0.2457
S_{18}-O_{20}	1.4643	H_7- C_{10}- C_{15}	120.0047	C_3- C_4- C_5-C_6	-0.1256
S_{18}-O_{21}	1.6497	C_4 -C_{11}-C_{14}	119.6476	C_3- C_4- C_5-12	179.9061
O_{21}-O_{22}	0.973	C_4 -C_{11}- H_{16}	120.3004	C_{11}- C_4- C_5-C_6	179.9469

Normally, C-C bond length in Naphthalene ring is not of the same length and the electron donating O-H group and electron withdrawing SO_3 group on the Naphthalene ring incline to contraction and elongation of C–C bond lengths adjacent to the substituent. Bond lengths are increased in the order C_1-C_2 (1.3741), C_1- C_6(1.4142),C_2-C_3(1.4178),C_3-C_4(1.431) since, C_3-C_{10}(1.4214),C_4-C_5(1.4188),C_4-C_{11}(1.4176),C_5-C_6(1.3733),C_{10}-C_{15}(1.3703),C_{11} C_{14} (1.3718), C_{14}-C_{15}(1.4146) are decreased respectively [11]. Bond length of S_{18}-O_{21} (1.6477Å) is higher than other S-O bond lengths S_{18}-O_{19} and (1.4509Å) and S_{18}-O_{20} (1.4573Å) which is due to the attachment of hydrogen atom with it. Bonding angles around sulfur atom depart slightly from tetrahedral arrangement which is manifested from its bond angles O_{19}-S_{18}-O_{20} (120.83°), O_{19}-S_{18}-O_{21} (108.55°), S_{18}-O_{21}-H_{22} (107.15°) and O_{20}-S_{18}-O_{21} (106.45°) [12]. In fact, the sulfoxide O_{19}-S_{18}-O_{21} and O_{20}-S_{18}-O_{21} indicates the pyramidal configurations of sulfonamide with benzene ring.

5. VIBRATIONAL SPECTRAL ANALYSIS

Vibrational band assignments have been performed based on Normal Coordinates Analysis. Non-redundant set of internal coordinates have been defined and used as data file to molvib program while the selective scaling has been incorporated according to the SQM scheme using a set of 14 transferable scale factors with RMS frequency error 8 cm^{-1}. Detailed spectral assignments with KNS contributions are tabulated in Table 2 and observed with simulated IR - Raman spectra are presented in Fig.3. Vibrational band assignments of the different functional groups analyzed in detail are discussed below:

5.1 C-H vibrations

Presence of aromatic structure shows C-H stretching vibration in the region 3100-3000 cm^{-1} which is the characteristic region for the identification of C-H stretching vibration [13]. KNS molecule has seven C-H bonds which include in-plane and out-of plane bending vibrations corresponding to C_1-H_8, C_2-H_9, C_{10}-H_7, C_{15}-H_{17}, C_{11}-H_{16}, C_5-$H_{12}$and C_6-H_{13} units respectively. FT-IR spectrum of NSA consists of very weak to very strong bands at 3064cm^{-1} and3005 cm^{-1}which are assigned to C-H stretching vibrations with its counterpart at 3063cm^{-1}. Stimulated wavenumbers by B3LYP/6-31G(d,p) method fall at 3055, 3046, 3041, 3029, 3021,3018 and 3013 $cm^{-1}$with PED contribution of 99% as shown in Table 2.

The C-H in-plane bending vibrations are usually expected to occur in the region 1300-1000 cm^{-1} and these vibrations are very useful for characterization purpose [14]. For KNS, a strong band at 1143cm^{-1} is observed in FT-IR spectrum and very weak bands at 1245, 1200 and 1141 cm^{-1} are in observed FT-Raman spectrum. The C-H out-of-plane bending vibrations are strongly coupled vibrations and occur in the region 1000-750 cm^{-1}[14]. Calculated aromatic C-H out-of-plane bending vibration fall at 947, 857, 815,781, 774 and 755 cm^{-1} by B3LYP/6-31G(d,p) method which shows good agreement with the recorded FT-IR band at 869, 813, 786 and 748 cm^{-1} and FT-Raman band at 943, 856 and 767cm^{-1} respectively as shown in Table 2. Computedas well as recorded spectral data are found to match very well withalready reported values [15, 16].

5.2 O–H vibrations

Hydroxyl group absorbs strongly in the region 3700-3584 cm^{-1}, whereas the existence of intermolecular hydrogen bond formation can lower the O-H stretching frequency in the range 3500-3200 cm^{-1} with increase in intensity[17, 18].In the title compound, strong band observed at 3396 cm^{-1} in FT-IR spectrum is assigned to O_{21}-H_{22} stretching vibration and the

computed value for this mode is at 3396 cm^{-1} as shown in Table 3which shows a deviation of about ~100 cm^{-1} due to the presence of intermolecular hydrogen bonding. Expected TED for this mode is a pure mode of 100%.O-H in-plane bending vibration generally lies in the region 1150-1250 $cm^{-1}$and is not much affected due to the hydrogen bonding unlike stretching and out-of-plane bending frequencies [19].In KNS molecule the band at 1159cm $^{-1}$,in FT-Raman spectrum is assigned to O_{21}–H_{22} in-plane bending vibration showing good correlation with computed wavenumber at 1159 cm^{-1} with TED contribution of 75%. O–H out-of-plane bending mode fall also below 300 cm^{-1} for the molecule without having intermolecular interaction and it is beyond the infrared spectral range for the associated molecules [14].

5.3 Sulfonic acid vibrations

Normally, SO_3 stretching vibrations are strongly IR active and appear in the region 1080-1209cm^{-1}, whereas the SO_3 symmetric deformation mode gives strong bands in the region 550-660cm^{-1}. [20, 21] Sulfonic group does not affect the conjugated system irrespective of the substitution position in the naphthalene rings. Changes in electron density are relatively low for carbon atoms where sulfonic groups are substituted. [22] Furthermore, the participation of sulphur d orbital in the conjugated system is very low, and the π contribution to C-S bond is practically negligible. Symmetric stretching mode of SO_3 is observed as a very strong band at 1084 cm^{-1}in IR and as a weak intensity band at 1097 cm^{-1}in Raman with the computed band at 1082 cm^{-1}which is in good agreement with observed values. The symmetric deformation is observed as a very weak IR band at 506 cm^{-1} and the stimulated band at 502 cm^{-1}. These vibrations are mixed with naphthalene ring deformations. SO_3 bending vibrations are coupled with the out-of-plane bending vibrations of naphthalene rings which appear as very weak intense bands in IR spectrum at 748 $cm^{-1}$and computed at 755 cm^{-1}. Weak intensity observed and computed bands in Raman spectrum at 354 cm^{-1} and 356 cm^{-1}correspond to SO_3 wagging vibrations. Weak bands at 261 cm^{-1} and 271 cm^{-1} in the Raman spectrum are assigned to SO_3 rocking vibrations, which are mixed with torsion vibrations of both naphthalene rings.

5.4 Skeleton Vibrations

Naphthalene ring vibrations are found to make a major contribution in the IR and Raman spectral vibrations. Naphthalene ring stretching vibrations are expected in the region 1620-1390 cm^{-1}. [23,24]Ring C-C stretching vibrations in the benzene ring appears in the range 1430-1625 cm^{-1}. In general, the bands are of variable intensity and are observed at1625-1590, 1590-1575, 1465-1430 and 1380-1280 cm^{-1} from the wave number range for the five bands in the regions. [14]For the title compound, computed wavenumbers byB3LYP/6311G(d,p) method are 1631, 1595, 1580, 1511, 1456, 1437, 1379, 1368, 1342, 1245, 1225, 1146, 1110,1033,1015 cm^{-1}.

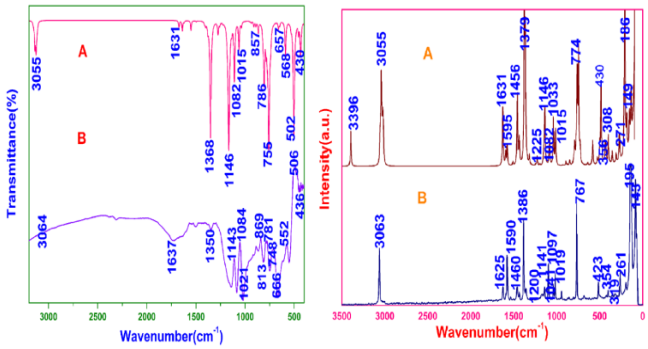

Figure.3 Experimental and simulated FT-IR and FT-Raman spectra of KNS.

Table 2: Vibrational assignment of KNS by Normal Coordinate Analysis based on SQM force field calculations.

Observed fundamentals/cm^{-1}		Selective scaled B3LYPwith 6-311G(d, P)force field	
ν_{IR}	ν_{Raman}	ν_{cal} cm^{-1}	Assignment with PED (≥10%)
3396s		3396	νOH (100)
3064vvvw	3063vs	3055	νCH_{R2}(99)
		3046	νCH_{R2}(98)
		3041	νCH_{R1}(98)
		3029	νCH_{R1}(98)
		3021	νCH_{R2}(87),νCH_{R1}(13)
		3018	νCH_{R1}(89), νCH_{R2}(10)
	3005vvw	3013	νCH_{R1}(97)
1637vvvw	1625vw	1631	νCC_{R1}(36), νCC_{R2}(29)
	1590vw	1595	νCC_{R2}(36), νCC_{R1}(33), βCH_{R1}(13), βCH_{R2}(11)
	1577s	1580	νCC_{R1}(43), νCC_{R2}(29)
	1503vw	1511	νCC_{R1}(30), βCH_{R1}(28), νCC_{R2}(26), βCH_{R2}(11)
	1460vw	1456	βCH_{R2}(38), βCH_{R1}(28), νCC_{R2}(18), νCC_{R1}(13)
	1433vw	1437	βCH_{R1}(42), νCC_{R1}(22), νCC_{R2}(20)
	1386s	1379	νCC_{R2}(58), νCC_{R1}(28)
1350w	1358vw	1368	νCC_{R1}(67), βCH_{R2}(11), βCH_{R1}(11)
		1342	βCH_{R2}(39), βCH_{R1}(26), νCC_{R2}(25)
		1306	ν_{IPS} SO_3(66), ν_{OPS} SO_3(19)
	1245vw	1245	βCH_{R1}(42), νCC_{R1}(23), $R2_{TRID}$ (12), νCC_{R2}(11)
	1200vw	1225	βCH_{R2}(49), νCC_{R2}(17), βCH_{R1}(12)
		1196	νCC_{R1}(33), νCC_{R2}(29), βCH_{R1}(25), βCH_{R2}(10)
	1159vw	1159	βOH (75),ν_{OPS} SO_3(13)
		1153	βCH_{R1}(60), νCC_{R1}(18), νCC_{R2}(12)
1143s	1141w	1146	βCH_{R2}(40), βCH_{R1}(22), νCC_{R1}(18), νCC_{R2}(18)
		1110	βCH_{R1}(24), νCC_{R1}(20), νCC_{R2}(16), $R2_{TRID}$(15), βCH_{R2}(15)
1084vs	1097w	1082	$\nu_S SO_3$(34), $\nu_{IPS} SO_3$(23), ν_{OPS} SO_3(22), βOH (15)
	1041w	1033	νCC_{R2}(66), βCH_{R2}(20)
1021vs	1019w	1015	νCC_{R1}(75), βCH_{R1}(18)
		953	$R2\tau_{ASYTO}$ (54), $R2_{Puck}$(20)
	943w	947	$R2\tau_{ASYTO}$ (51), $R2_{Puck}$(21), gCH_{R1}(12)
		924	gCH_{R1}(59), $R2_{Puck}$(21)
		906	$R2_{Puck}$(57), $R2_{ASYT}$(19), gCH_{R2}(14)

Recorded IR and Raman spectrum shows bands of medium to very strong intensity at 1637, 1625, 1590, 1577, 1503, 1460, 1433, 1386, 1350,1358,1245,1200,1159,1141,1041and 1019

cm^{-1}.The in-plane deformation vibrations are at higher wave number than the out-of-plane vibrations and computed values of ring vibrations shows good agreement with recorded spectral data.

6. ELECTRONIC SPECTRA

Electronic transitions are mainly derived from the contribution of bands π - π*. UV-vis absorption spectrum of the sample dissolved in D_2O is shown in Fig.4.The maximum absorption values at 309 and 302 nm are computed at 307 and 299 nm. Experimental band at 309 nm is attributed mainly to HOMO→LUMO transition with 74% contribution. This transition is predicted as π→π* transition.Gauss Sum 2.2 program [25] was used to calculate group contributions the density of states (DOS) spectra in Fig.5. DOS spectra were created by convoluting the molecular orbital information with GAUSSIAN curves of unit height. Calculations of the electronic structure of KNS molecule were optimized in singlet state. Other wavelength assignments and calculated counterparts with major contributions are presented in Table 3 Electronic absorption peak at 309 nm corresponds to the transition from the ground to first excited state and it is mainly described by one electron excitation from the HOMO→LUMO (π→π*). Observed wavelength in the UV spectrum is higher than calculated wavelength and this difference is observed due to bathochromic shift (red shift). These transitions are of lower energy. The bathochromic shift occurs due to hydrogen bonding of the solvent effect.In the present case the energy transitionsare in reasonable agreement with experimental results. Optical band gap of KNS is found to be 4.7eVwith computed HOMO→LUMOenergy gap as 4.7eV which is in good agreement.

Table.3 UV–vis excitation energy and oscillator strength for KNS

No.	Exp.Wave length(nm)	Cal.Wave length(nm)	Energy(eV)	Osc.Strength	Symmetry	Major contributes
1	309	307	34362.68224	0.0386	Singlet-A	H-1->LUMO (10%), HOMO->LUMO (74%)
2	302	299	36252.45232	0.0121	Singlet-A	H-1->LUMO (38%), HOMO->LUMO (19%), HOMO->L+1 (42%)
3		217	45945.6904	0.6458	Singlet-A	H-2->LUMO (36%), H-1->LUMO (29%), HOMO->L+1 (23%)
4		216	46252.98976	0.1793	Singlet-A	H-3->LUMO (28%), H-2->LUMO (20%), HOMO->L+2 (34%)
5		213	46938.56576	0.2438	Singlet-A	H-3->LUMO (31%), H-2->LUMO (35%), H-1->L+1 (11%)
6		206	48508.13152	0.2789	Singlet-A	H-3->LUMO (10%), H-1->L+1 (66%)

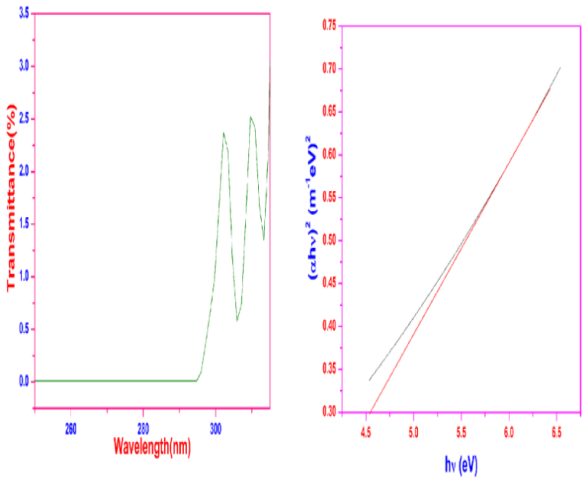

Fig. 4 UV-Vis.Transmittance Spectrum and (αhν) vs. photon energy (hν).

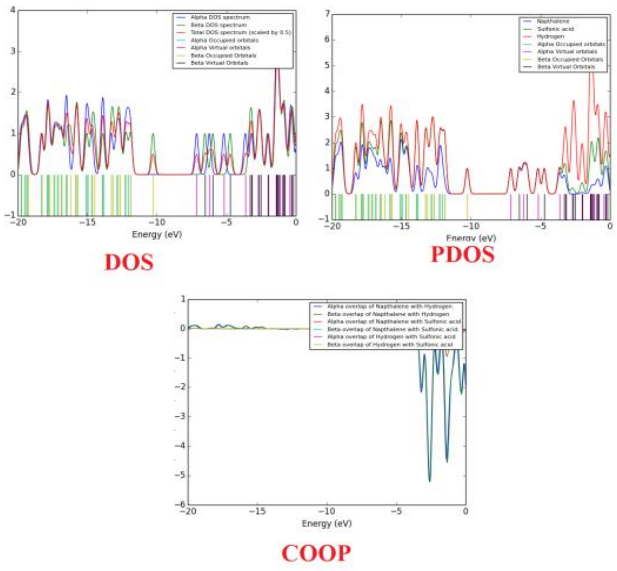

Fig.5 DOS, OPDOS and COOP diagrams.

7. ANTIMICROBIAL ACTIVITY

Antimicrobial activity testing was performed by Kirby-Bauer method and the activity against bacterial strains were photographed and shown in Fig.6&7 and Table 4.shows the zone of inhibition of bacterial strains. Biological evaluation of KNS showed momentous antibacterial activity against gram-positive bacteria *Pseudomonas aeruginosa* with zones of inhibition (18 mm)but gram-positive bacteria *Staphylococcus aureus*, *Proteus mirabilis* and the gram-negative bacteria *Escherichia coli*. Moreover it is found that KNS exhibits higher antibacterial activity for the bacterial strain Pseudomonas wherein it shows highest activity against other bacterial strains.

Table.4 Antibactrial Activity of KNS

	Control	1/1ml	1/20ml	1/40ml
Escherichia coli	30	10	12	10
Staphylococcus aureus	27	11	11	12
Proteus mirabilis	26	10	13	10
Pseudomonas aeruginosa	21	7	18	21

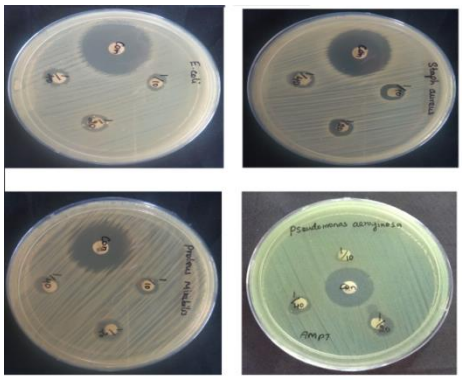

Fig.6 Photographs of antimicrobial activity

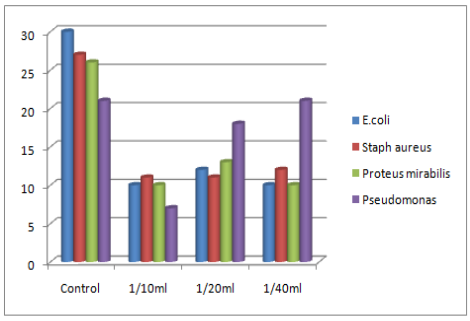

Fig. 7 Bar diagram of antimicrobial activity

7.1 Molecular Docking

Molecular modeling, used to explore the binding mode of the macromolecules, was performed using Auto Dock Tools available in free software package UCSF chimera [26]. KNS was preferred to be docked into bioactive site of different receptors 1VAI, 1JZS, 3U2D, and 1JZQ which were obtained from Protein Data Bank (PDB). KNS ligand obtained from Gaussian were docked into the functional sites of the respective proteins independently and the docking energy was monitored to accomplish a minimum value. Protein- ligand interactions with their binding affinity, RMSD for different interaction within the binding site as well as hydrogen bond distances. Values obtained for protein targets clearly shows that KNS has bonded effectively with 1JZQ target sites with four hydrogen bonds (2.0 Å , 1.9 Å, 1.7 Å, and 1.7 Å) with estimated inhibition constant 25.71 µM. Hydrogen bonds formed with corresponding proteins 1VAI (2.2 Å) 1JZS (1.7 Å) and 3U2D (2.2 Å,2.0 Å) indicates that hydrophobic forces play an essential role in the hydrogen bonds. Binding mode obtained from KNS against 1VAI, 1JZS, 3U2D, and 1JZQ proteins are given in Fig.8 which shows that KNS molecule is highly bonded with target proteins showing mutual complement between spectroscopy techniques and binding affinity providing fruitful biological information about the interaction and conformation of adduct from different aspects.

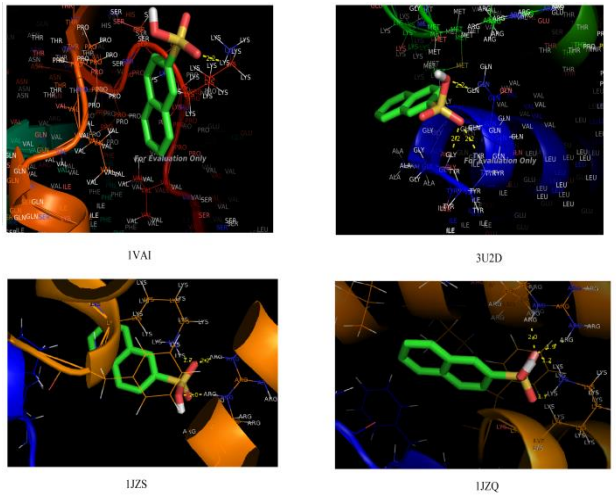

Fig.8 KNS docked into the binding site of1VAI, 1JZS, 3U2D, and 1JZQ.

8. CONCLUSION

Investigations performed on KNS reveals that it has wide biological applicationsand hence spectroscopic investigation along with quantum chemical computations has been performed to illustrate its spectroscopicimplication, charge transfer interactions and biological activity.Optimized geometry and vibrational wavenumbers of NSA have been analyzed with the aid of density functionaltheory method with B3LYP/6-311++G (d,p) level basis set. The variousmodes of vibrations are assigned on the results of PED outputobtained from the normal coordinate analysis. Calculated wavenumbers are in good agreement with the experimental results.HOMO→LUMOenergy gap value of 4.7eVsuggests the possibility of charge transfer in the molecule making it a suitable bioactive molecule. Docking results suggest that KNS molecule has greater binding affinity towards antimicrobial

proteins that is clearly depicted from molecular visualization tool.

REFERENCES

[1] Abdelkarim Guaadaoui, Soumaya Benaicha, Naima Elmajdoub, Mohammed BellaouI, Abdellah Hamal ,International Journal of Nutrition and Food Sciences 2014; 3(3): 174-179 .
[2] Storm, T., Reemtsma, T., Jekel, J.,. J. Chromatogr. A 854, 175–185(1999).
[3] Suter, M.J.F., Riediker, S., Giger, W., Anal. Chem.71, 897–904(1999).
[4] Riediker, S., Suter, M.J.F.,Giger, W. Water Res.34, 2069–2079(2000).
[5] M. J. Frisch *etal. Gaussian 09, Revision D.01*, Gaussian, Inc.,Wallingford CT, (2010).
[6] T. Sundius, Vib. Spectrosc. 29 (2002) 89–95.
[7] T. Sundius, J. Mol. Struct. 218 (1990) 321.
[8] P. Pulay, G. Fogarasi, G. Pongor, J.E. Boggs, A. Vargha, J. Am. Chem. Soc. 105(1983) 7037.
[9] P. Pulay, G. Fogarasi, F. Pang, J.E. Boggs, J. Am. Chem. Soc. 101 (1979) 2550.
[10] G.M. Morris, R. Huey, W. Lindstrom, M.F. Sanner, R.K. Belew, D.S. Goodsell, A.J.Olson, J. Comput. Chem. 16 ,2785(2009).
[11] H.L. Cheng, S.Q. Zhang, C.F. Huang, ActaCrystallogr. E63 (2007) 1979–1980.
[12] ChithraNeelakanda Pillai & James Chellapan J Mol Model (2014) 20, 2139
[13] G. Varsanyi, Assignments for Vibrational Spectra of Seven Hundred BenzeneDerivatives, vols. 1–2, Academic Kiacio, Budapet, 1973.
[14] G. Thilagavathi, M. Arivazhagan, Spectrochim. Acta 79A (2010) 389–395.
[15] M. Karabacak, E. Postalcilar, M. Cinar, Spectrochim. Acta 85A (2012) 261–270.
[16] M. Arivazhagan, S. Prabhakaran, R. Gayathri, Spectrochim. Acta A82 (2011)323–339.
[17] B. Smith, Infrared Spectral Interpretation, A systemic Approach, CRC Press,Washington, DC, 1999.
[18] R.M. Silverstein, F.X. Webster, Spectroscopic Identification of Organic Compounds, sixth ed., John Wiley & Sons, Inc., New York, 2003.
[19] D. Michalska, D.C. Bienko, A.J.A. Bienko, Z. Latajka, J. Phys. Chem. 100 17786–17790(1996).
[20] Sperline R, Song Y, Freiser H. Langmuir; 10: 37(1994).
[21] Hanai K. Spectrochim. Acta; 49A: 1131(1993).
[22] Wojciechowski K, Jerzy S. Dyes Pigments; 44: 137(2000).
[23] C. Surisseau, P. Marvel, J. Raman Spectrosc. 25, 447–455(1994).
[24] A.J. Barnes, M.A. Majid, M.A. Stuckey, P. Gregory, C.V. Stead, Spectrochim. Acta41A ,629–635(1985).
[25] N.M. O'Boyle, A.L. Tenderholt, K.M. Langer, J. Comput. Chem. 29,839–845(2008).
[26] A. Grosdidier, V. Zoete, O. Michielin, Nucleic Acids Res. 39, W270–W277,(2011).